Available online at www.sciencedirect.com
SCIENCE DIRECT
Marine Chemistry 100 (2006) 39–52
MARINE CHEMISTRY
www.elsevier.com/locate/marchem

Rare earth elements in the modern sediments of the Bay of Biscay (France)

Gwénaëlle Chaillou *, Pierre Anschutz, Gilbert Lavaux, Gérard Blanc

Université Bordeaux I, Environnements Paléoenvironnements Océaniques (EPOC), UMR-CNRS 5805, Avenue des Facultés, 33405 Talence Cedex, France

Received 26 January 2003; received in revised form 8 September 2005; accepted 12 September 2005
Available online 25 January 2006

Abstract

Particulate rare earth elements (REEs) were measured in modern sediment from the Bay of Biscay. Vertical profiles of total and reactive (ascorbate reducible) REEs have been studied in four contrasted sites ranging at water depth from 150 to 2800 m. The focus is on the coupling between the diagenetic conditions and the behavior of particulate REE.

Total REEs fraction appears to be affected by the presence of metal sulphides that may act as an important carrier phase for solid REEs. In sediments where sulphate reduction is weak, the transfer from an unknown previous phase, stable in oxic conditions, to another one associated with sulphides seems to be direct, without mobilization in porewaters. In sediments where greater sulphate reduction occurs, we note the formation of an additional "authigenic" phase. Consequently, a threshold level of dissolved sulphide is a prerequisite for the formation of an additional "authigenic" REEs fraction. No direct relationship between the REE_{asc} profiles and authigenic metal oxides have been observed, indicating that authigenic Fe and Mn oxides do not act as an efficient traps in the sediment. Despite particulate REE are mobile in these sediments, no fractionation of the lanthanide series is observed in relation to the redox conditions.

Keywords: Rare earth elements; Diagenesis; Modern sediment; Bay of Biscay

1. Introduction

Crustal contents, distribution patterns, and isotopic signature of rare earth elements (REEs) have been widely employed as geochemical tracers in the marine environment (Piper, 1974; Broecker and Peng, 1982; Elderfield, 1988; Tachikawa et al., 1999). REEs are useful for determining petrogenetic histories of rock suites (Shields and Stille, 2001), monitoring detrital sediment sources (Grousset et al., 1998), and elucidating seawater circulation patterns (Tachikawa et al., 1999), hydrothermal fluxes (German et al., 1999), and past oxygenation of the oceans (Henderson, 1984; Murray et al., 1992). For these tracers to be useful, it is essential to understand the sources and sinks of REEs in the ocean and their mobility after deposition on the sea floor.

The major sources of REE to the ocean are fluvial suspended sediments, atmospheric dust (Elderfield and Greaves, 1982), and hydrothermal vent exhalations (Fleet, 1984; Goldstein and Jacobsen, 1987; Olivarez and Owen, 1991). Dissolved fluvial REEs are rapidly removed during mixing with seawater in estuaries, and are largely adsorb on Fe-organic colloids (Sholkovitz and Elderfield, 1988; Elderfield et al., 1990; Sholko-

* Corresponding author. McGill University, Earth and Planetary Sciences, 3450 University Street, Montréal, QC H3A 2A7, Canada.
E-mail address: chaillou@eps.mcgill.ca (G. Chaillou).

0304-4203/$ - see front matter © 2006 Published by Elsevier B.V.
doi:10.1016/j.marchem.2005.09.007

vitz, 1993) and particulate organic carbon (Byrne and Kim, 1990; Sholkovitz, 1992; Schijf et al., 1995; Arraes-Mescoff et al., 2001; Haley et al., 2004). REEs passing into the open ocean may be altered by post-depositional or redox processes linked to the mineralization of organic matter in modern sediments (Elderfield and Pagett, 1986; German et al., 1991; Haley et al., 2004).

Although McLennan (1989) concluded that REEs mobility is insignificant during sediment burial, few data exist on the diagenetic fate of REEs in modern sediments. This study examines the vertical distribution of particulate REEs in four sediment cores which represent oxic to anoxic sedimentary environments. Total and extractable REEs are compared to major components of the redox system which could alter REE distribution.

2. Samples and methods

2.1. Sampling

The Bay of Biscay is a semi-enclosed basin on the eastern side of the Northern Atlantic Ocean, bathed by homogenous oceanic waters from the North Atlantic Drift. Several rivers in France and Spain (Loire, Charente, Gironde, Adour, Bidassoa, and Ebre) feed the sedimentary basin. The Gironde and Loire Rivers are presently the main sources of fine sediments to the margin (Thomas et al., 1994).

Undisturbed sediment cores were collected in June 1999 at four sites in 150 and 2800 m water depths in the south-eastern part of the Bay of Biscay on the slope of the Aquitaine margin (stations A, B, and D) and close to the Cap Ferret canyon (station I; Fig. 1). Cores were collected with a multicorer, which allowed us to sample the sediment–water interface with minimum disturbance. Overlying water was collected immediately after core recovery for dissolved O_2 measurements using the Winkler method (Strickland and Parsons, 1972). Vertical profiles of O_2 in sediment porewater were measured on board ship using a cathode-type mini-electrode (Revsbech, 1983) while keeping the cores at bottom water temperature using an insulating device. The profiling was completed within 15–30 min after core recovery. The core used for O_2 profiling was then sliced in thin horizontal sections (0.5 cm for the top 2 cm, 1 cm below, and 2 cm near the bottom). This took less than 90 min. A sub-sample of each slice was immediately sealed in a pre-weighed vial and frozen under an inert atmosphere (N_2) for later determination of porosity. Another sub-sample was centrifuged under

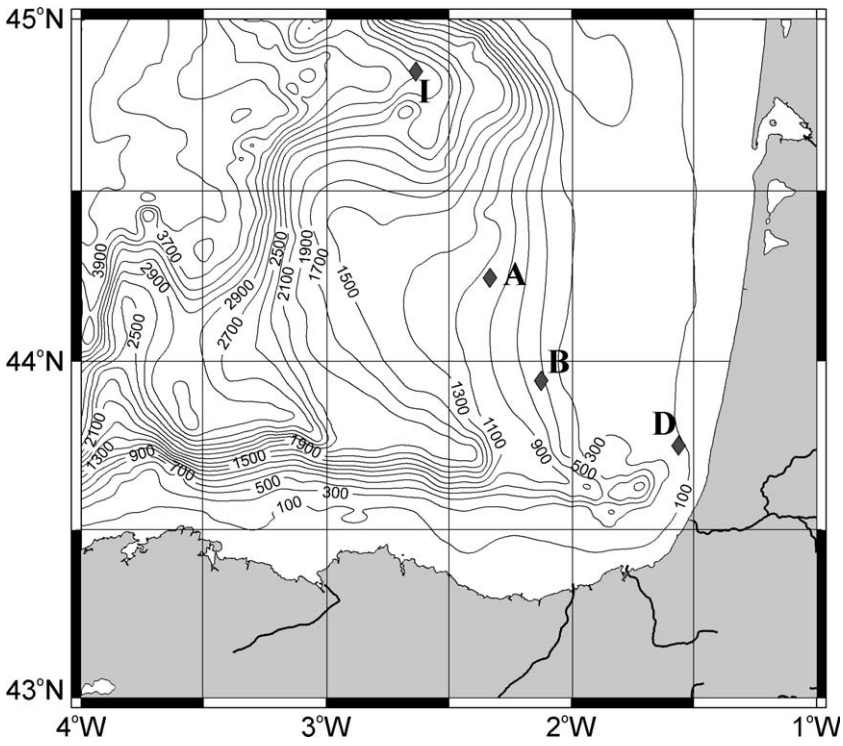

Fig. 1. Map of the southern part of the Bay of Biscay showing the locations of Oxybent 9 cruise stations.

N_2 at 5000 rpm for 20 min to extract porewater. The supernatant was immediately filtered (0.2 μm, syringe filter SFCA Nalgene® purged by N_2), and acidified (HNO_3; s.p.) for dissolved Fe and Mn analysis or frozen for nutrient analysis. A second tube of the same multicore deployment was sampled for radioisotope and grain size analyses.

2.2. Analyses

2.2.1. REEs, manganese, and iron

Total sediment digests were prepared according to the procedure of Loring and Rantala (1992). Thirty milligrams of freeze-dried sediment were weighed and added to 2 ml HF, 250 μl HNO_3 70% and 750 μl HCl 30% in Savillex® Teflon beakers. The samples were refluxed on a hot plate at 110 °C for 2 h. After cooling to room temperature, beakers and caps were rinsed with nanopure H_2O to concentrate the digestates in the bottom of the beakers. The solutions were then evaporated to dryness at ~100 °C for 12 h. The resulting crusts were taken up in 250 μl HNO_3 70% and 5 mL of nanopure H_2O and diluted to obtain 10 ml of 1% HNO_3 with a water/rock ratio close to 500. Particulate metals and REEs were also leached with an ascorbate solution to extract the most reductive Fe (III)-phases and Fe-monosulphides, all Mn(III, IV)-oxides, and associated REEs (Kostka and Luther, 1994; Anschutz et al., 1998). For this procedure, about 1 g of wet sediment was leached for 24 h with 25 ml of the ascorbate solution (50 g of $NaHCO_3$, 50 g of Na-citrate, 20 g of ascorbic acid for 1 L solution; buffer at pH 8). The supernatant was diluted with 0.2 M HCl for Fe and Mn analysis and with 1% HNO_3 solution for REE analysis. All acids were of suprapur quality.

Iron and manganese were analyzed using flame atomic absorption spectrometry (Perkin Elmer AA 300). The precision was ± 3% for Mn and ± 5% for Fe. Accuracy was better than 10%. The concentrations of REEs were determined using an inductively coupled plasma-mass spectrometer (ICP-MS Elan 5000, Perkin Elmer). The specific REE isotopes to analyze were chosen on the basis of their natural abundances, non-isobaric overlap with other elements in the sample, and the absence of polyatomic ion interferences caused by precursors in the plasma gas and in the sample matrix. The following isotopes were chosen: ^{139}La, ^{140}Ce, ^{141}Pr, ^{146}Nd, ^{147}Sm, ^{153}Eu, ^{157}Gd, ^{159}Tb, ^{163}Dy, ^{165}Ho, ^{166}Er, ^{169}Tm, ^{174}Yb, and ^{175}Lu. Samples without sediment were subjected to same digestion procedures as an analytical "blank", which was below the detection limit for all the analyzed compounds. The applied analytical methods were continuously quality checked by parallel analysis of international certified reference materials (MESS-2, SL-1, and NIST 1646). The precision was generally better than 3%. To provide the validity of our measures the same sediment sample was analyzed 15 times in succession. The accuracy was better than 1.5%.

2.2.2. Others species and parameters

Dissolved REEs were not measured because of the small sample volume. Sulphate was analyzed with a nephelometric method (AFNOR, 1997) with precision better than 2%.

Activity of ^{210}Pb was determined on freeze-dried samples by gamma counting. Excess ^{210}Pb activity was calculated from ^{226}Ra-supported ^{210}Pb deduced from ^{214}Pb and ^{214}Bi activities. Grain size distribution was measured using a laser diffractometer (Malvern Mastersizer).

3. Results and discussion

3.1. Lithologic features of the studied sediments

The sediments consisted of fine-grained mud with mean grain size of 9–11 μm. Fine silt and clay fraction (<15 μm) represents ~70% of sediments at the two deepest stations (A and I; Fig. 1), ~60% at the station B, and ~50% at the shallowest station (D; Fig. 1). The grain size distribution is linked to the distance from the sediment source. Illite represents between 50% and 70% of the clay fraction (Tauzin, 1974; Latouche et al., 1991). Kaolinite, chlorite, and smectite concentrations make up 10–20%. The clay composition was constant in a given core. Clay minerals are known to be highly efficient in retaining trace metals, radionuclides, and contaminants. REEs are mainly adsorbed on the clay fraction in argillaceous sediments (Balashov and Girin, 1969; Aagaard, 1974; Sinitsyn et al., 2000).

The excess ^{210}Pb activity decreased exponentially below the interface at the deep slope stations (I, A, and B; Fig. 2). The $^{210}Pb_{xs}$ activities of surface sediments measured in cores from this cruise were close to those measured during previous cruises, which suggests that the flux is constant (Hyacinthe et al., 2001). There was no detectable peak of $^{210}Pb_{xs}$-activity in the bottom sediments, and the X-ray images of the sediment cores collected at the same locations indicated the absence of slumping or turbiditic structures (data not shown). These data confirm the absence of sedimentary events and suggest that bioturbation is not important in the deepest cores (i.e. B, A, and I). For these sites, we can assume steady-state conditions and use the depth

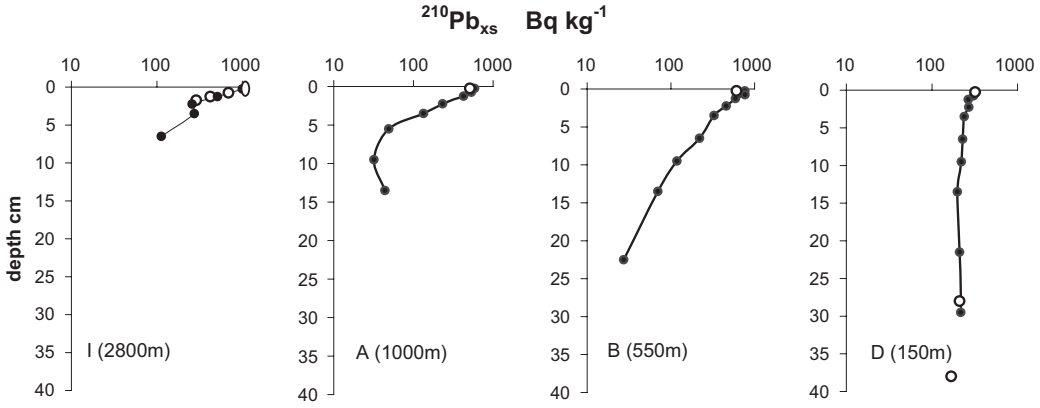

Fig. 2. Vertical profiles of log $^{210}Pb_{xs}$ in Bq/kg. The $^{210}Pb_{xs}$ profiles of stations I, A, B, and D (black dots) were obtained from cores collected during the mission Oxybent 1 (October 1997). The open dots (○) represent the log $^{210}Pb_{xs}$ of surface sediments collected during Oxybent 9 (June 1999).

distribution of $^{210}Pb_{xs}$ to estimate recent sedimentation rate. The maximum rates deduced from the slopes of the $^{210}Pb_{xs}$ profiles, and the radioactive decay constant, are 0.033, 0.068, and 0.15 cm year^{-1} for stations I, A, and B, respectively.

The $^{210}Pb_{xs}$ activity was almost constant at station D with only a small decrease from 320 to 168 Bq/kg at 40 cm depth (Fig. 2). The X-ray image of the station D shows unlaminated sediment, and there is no evidence of slumping structures. However macrofaunal structures were observed down to the bottom of the sediment section, suggesting strong biological activity deep below the sediment surface. The presence of polychaetes and numerous active burrows down to several decimeters depth at this station, further support this hypothesis.

3.2. Vertical changes in redox state

The C_{org} content of these surface sediments decreased from the shallowest station D (2.32%, Table 1) to the deepest station I (1.39%). At stations I, A, and B, the C_{org} content decreased slowly down core. It remained approximately constant at station D. Chaillou et al. (2002) estimated that the C_{org} flux at the sediment–water interface decreases as D≫B>A>I.

The bottom water is well oxygenated at all the sites (Table 1). O_2 penetration depths in the sediment range from 5 mm at the shallowest station D to 50 mm at the deepest station I (Fig. 3). The distributions of major redox species follow the same pattern in the four cores (see Chaillou et al., 2002). The oxygen concentration decreased rapidly below the sediment surface (Fig. 3). Nitrate increased in the oxygen containing layer and then decreased below the O_2 front (Chaillou et al., 2002). The disappearance of oxygen and nitrate was

Table 1
Some properties of the studied stations (Oxybent 9)

	Station I	Station A	Station B	Station D
Geographic position	44°49′00N 2°33′00W	44°10′00N 2°22′00W	43°50′00N 2°03′00W	43°42′00N 1°34′00W
Depth (m)	2800	1000	550	150
Temperature (°C)	4	12	12	12.5
O_2 bottom water (μmol l^{-1})	253	200	215	235
$\%C_{org}$ interface	1.39	1.51	1.83	2.32
$\%C_{inorg}$ interface	2.75	3.37	2.12	1.59
Maximum sedimentation rate (cm year^{-1})	0.033	0.068	0.15	

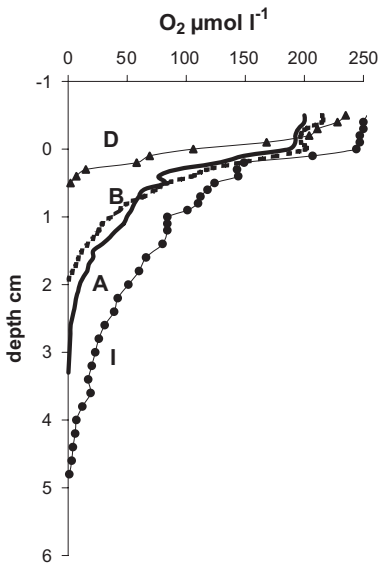

Fig. 3. Porewater profiles of oxygen in μmol l^{-1} vs. depth at stations D (150 m), B (550 m), A (1000 m) and I (2800 m). The water–sediment interface is located at 0 cm.

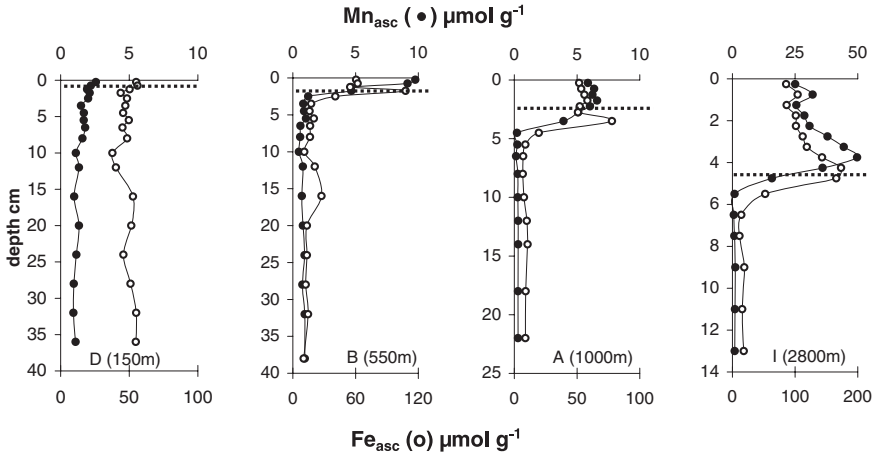

Fig. 4. Concentrations (in µmol g^{-1}) of Mn (●) and Fe (○) extracted by ascorbate vs. depth at stations D (150 m), B (550 m), A (1000 m) and I (2800 m). Dashed lines represent the depth of the O_2 front.

accompanied by a decline in the Mn and Fe oxide content (Fig. 4), and by an increase in Mn and Fe in the porewaters below the oxic front (Chaillou et al., 2002). At each of the four stations, the lowest total sulphur (S_{tot}) concentrations occurred in the sediment surface layer. The cores from stations I, A, and B showed relatively constant S_{tot} concentrations with values below 30 µmol g^{-1} (Fig. 5). A slight decrease of the S_{tot}-content (<10 µmol g^{-1}) is observed in the bottom part of the core A (below 14 cm, Fig. 5). The presence of particulate S in continental margin sediments is often attributed to authigenic iron sulphide minerals, formed during organic carbon mineralization by sulphate reduction (Berner, 1970; Jørgensen, 1982). The first authigenic compound formed during this reduction step is generally amorphous FeS, which is slowly converted to more crystalline FeS_2 in the presence of sulphides (Jørgensen, 1982). Previous studies (Chaillou et al., 2002, 2003) confirmed the presence of Fe-monosulphides at station D by the sediment's black colour below 5 cm, the characteristic odour of H_2S emanating during a HCl leaching and the profile of HCl-extractable Fe. These observations suggest sulphides production is more important at station D than at the deepest stations. The decrease of porewater SO_4^{2-} at the bottom of the core confirms the importance of sulphate reduction (Fig. 5).

The concentration profiles described above are consistent with the well-established depth sequence of

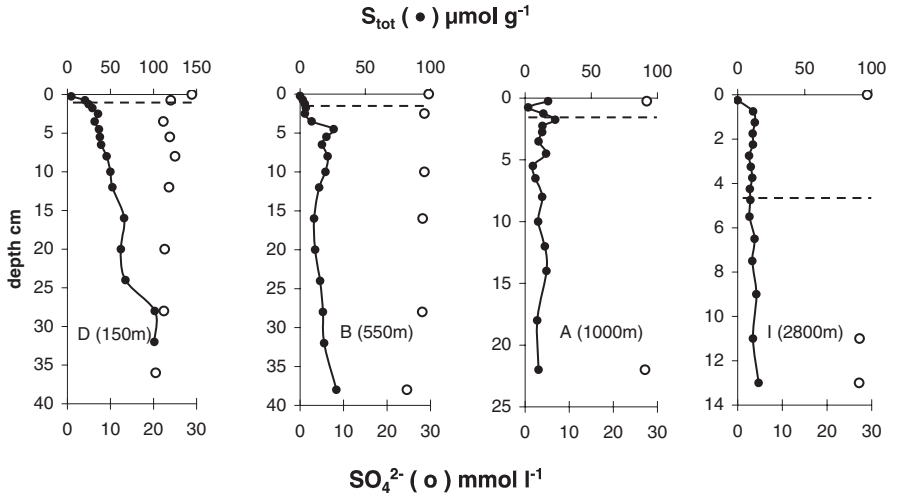

Fig. 5. Distribution of porewater sulfate (○) in mmol l^{-1} and total solid sulfur (●) in µmol g^{-1} vs. depth at stations D (150 m), B (550 m), A (1000 m) and I (2800 m). Dashed lines represent the depth of the O_2 front.

Table 2
Results of total particulate REEs ($REEs_{tot}$) in μg/g in the modern sediments of the Bay of Biscay and mean values of the North American shale composite in μg g^{-1}

	Depth (cm)	La	Ce	Pr	Nd	Sm	Eu	Gd	Tb	Dy	Ho	Er	Tm	Yb	Lu
NASC		30.00	65.00	6.70	27.00	5.30	1.30	4.00	0.65	3.80	0.80	2.10	0.30	2.00	0.35
Station D	0.25	14.29	29.22	3.50	13.73	2.60	0.66	2.42	0.33	1.76	0.33	0.96	0.13	0.87	0.13
	0.75	19.36	40.00	4.66	18.00	3.52	0.81	3.39	0.46	2.30	0.44	1.22	0.17	1.13	0.18
	1.25	17.90	37.54	4.37	16.84	3.17	0.77	3.00	0.44	2.11	0.43	1.16	0.18	1.03	0.17
	1.75	15.45	32.27	3.87	14.75	2.99	0.71	2.83	0.40	1.92	0.39	1.03	0.14	0.99	0.14
	2.50	25.43	51.79	6.24	23.39	4.59	1.02	4.29	0.61	2.94	0.54	1.58	0.21	1.45	0.21
	3.50	23.85	48.51	5.86	21.91	4.30	0.96	4.02	0.57	2.75	0.50	1.47	0.20	1.36	0.20
	4.50	20.73	40.98	4.84	18.46	3.55	0.83	3.42	0.46	2.53	0.42	1.25	0.18	1.19	0.17
	5.50	21.77	44.67	5.24	20.44	4.09	0.97	3.85	0.58	2.67	0.57	1.51	0.25	1.31	0.24
	6.50	24.70	51.68	6.04	23.53	4.91	1.15	4.50	0.62	3.22	0.60	1.68	0.24	1.49	0.22
	8.00	18.97	40.03	4.91	18.75	3.78	0.92	3.53	0.49	2.57	0.48	1.37	0.19	1.22	0.17
	10.00	21.35	44.83	5.07	20.55	4.08	0.96	3.82	0.53	2.70	0.52	1.50	0.20	1.33	0.20
	12.00	22.59	44.81	5.16	20.71	4.24	0.93	3.92	0.55	2.75	0.51	1.51	0.21	1.31	0.20
	16.00	24.54	50.56	5.94	23.24	4.65	1.15	4.44	0.67	3.09	0.59	1.72	0.28	1.56	0.26
	20.00	20.74	41.70	5.19	19.75	4.10	0.96	3.77	0.54	2.68	0.50	1.45	0.22	1.42	0.19
	24.00	21.42	42.93	5.23	19.85	3.75	0.89	3.52	0.50	2.70	0.49	1.41	0.20	1.24	0.18
	28.00	17.30	34.78	4.19	16.10	3.09	0.73	3.28	0.40	2.02	0.37	1.12	0.16	1.02	0.15
	32.00	26.12	53.70	6.33	24.19	4.75	1.17	4.66	0.64	3.25	0.61	1.78	0.23	1.53	0.22
	38.00	23.64	48.85	5.74	21.73	4.31	1.03	4.22	0.59	2.98	0.58	1.68	0.25	1.45	0.23
Station B	0.25	20.76	40.05	5.01	18.76	3.67	0.83	3.33	0.45	2.36	0.41	1.18	0.17	1.16	0.16
	0.75	27.27	53.75	6.41	24.42	4.84	1.10	4.28	0.60	2.94	0.53	1.59	0.22	1.47	0.22
	1.25	23.48	46.05	5.49	21.03	4.05	0.88	3.69	0.49	2.47	0.48	1.43	0.20	1.29	0.18
	1.75	22.71	44.79	5.39	20.05	3.92	0.91	3.69	0.49	2.36	0.46	1.32	0.18	1.25	0.18
	2.50	24.31	49.01	5.74	22.17	4.36	1.00	4.07	0.53	2.57	0.52	1.41	0.22	1.37	0.26
	3.50	23.95	46.44	5.59	23.65	4.33	1.00	4.17	0.57	2.67	0.51	1.47	0.21	1.43	0.21
	4.50	24.06	48.03	5.68	21.82	4.17	0.92	3.93	0.49	2.47	0.50	1.30	0.20	1.24	0.18
	5.50	23.70	46.57	5.59	21.16	4.14	0.97	3.91	0.52	2.54	0.52	1.47	0.20	1.35	0.19
	6.50	24.06	49.17	5.81	22.26	4.46	1.03	4.11	0.56	2.74	0.52	1.52	0.22	1.43	0.22
	8.00	23.44	46.92	5.76	21.97	4.16	0.95	3.78	0.53	2.56	0.56	1.38	0.25	1.49	0.23
	10.00	27.66	56.50	6.56	24.96	4.70	1.04	4.46	0.57	3.01	0.58	1.66	0.24	1.51	0.23
	12.00	23.62	46.42	5.56	21.57	4.22	0.89	3.68	0.49	2.52	0.48	1.41	0.19	1.29	0.19
	16.00	23.93	46.33	5.73	21.87	4.03	0.93	3.65	0.51	2.47	0.46	1.38	0.20	1.26	0.18
	20.00	27.44	54.91	6.41	24.56	4.54	0.99	4.22	0.54	2.73	0.50	1.53	0.20	1.45	0.20
	24.00	24.10	47.86	5.78	21.88	4.12	0.95	3.85	0.57	2.48	0.50	1.51	0.23	1.42	0.21
	28.00	24.97	48.98	5.84	22.00	4.29	0.97	3.86	0.52	2.73	0.51	1.48	0.22	1.38	0.21
	32.00	24.17	46.75	5.56	21.88	4.30	0.91	3.64	0.51	2.42	0.47	1.40	0.20	1.27	0.19
	38.00	21.17	41.66	4.96	19.44	3.62	0.87	3.45	0.48	2.39	0.45	1.44	0.23	1.25	0.18
Station A	0.25	17.77	34.45	4.25	16.09	3.10	0.68	2.80	0.35	1.86	0.37	1.05	0.15	0.95	0.13
	0.75	21.38	43.02	5.16	19.38	3.71	0.82	3.34	0.44	2.16	0.41	1.25	0.16	1.12	0.16
	1.25	14.18	27.94	3.37	12.83	2.44	0.54	2.08	0.29	1.54	0.27	0.84	0.11	0.88	0.09
	1.75	21.13	39.72	4.99	18.61	3.58	0.79	3.28	0.41	2.14	0.38	1.23	0.16	1.20	0.14
	2.25	10.06	19.88	2.36	9.40	1.78	0.42	1.60	0.26	1.14	0.27	0.67	0.13	0.64	0.12
	2.75	8.01	16.87	1.96	7.68	1.44	0.32	1.31	0.17	0.93	0.17	0.52	0.07	0.44	0.06
	3.50	23.29	44.68	5.68	21.39	3.96	0.88	3.71	0.48	2.45	0.50	1.36	0.19	1.31	0.21
	4.50	14.64	27.56	3.32	12.81	2.36	0.53	2.34	0.28	1.55	0.28	0.91	0.11	0.78	0.10
	5.50	20.62	39.97	4.95	19.47	3.62	0.78	3.42	0.45	2.42	0.46	1.33	0.17	1.25	0.16
	6.50	16.88	33.00	3.96	15.41	2.86	0.69	2.74	0.40	1.93	0.41	1.08	0.16	0.97	0.15
	8.00	15.69	28.61	3.55	13.38	2.57	0.55	2.38	0.28	1.50	0.29	0.88	0.12	0.76	0.10
	10.00	15.45	29.59	3.56	13.36	2.49	0.61	2.49	0.31	1.58	0.30	0.91	0.12	0.84	0.11
	12.00	14.39	28.52	3.62	13.47	2.56	0.55	2.39	0.36	1.60	0.29	0.91	0.12	0.87	0.09
	14.00	11.51	21.59	2.67	10.24	2.04	0.42	1.77	0.23	1.21	0.22	0.65	0.09	0.61	0.07
	18.00	7.47	14.26	1.81	7.32	1.30	0.29	1.21	0.18	0.79	0.15	0.40	0.07	0.35	0.06
	22.00	7.03	12.80	1.74	6.53	1.19	0.25	1.06	0.13	0.64	0.12	0.38	0.05	0.33	0.04

Table 2 (*continued*)

	Depth (cm)	La	Ce	Pr	Nd	Sm	Eu	Gd	Tb	Dy	Ho	Er	Tm	Yb	Lu
Station I	0.25	21.79	42.83	5.20	19.73	3.77	0.88	3.44	0.48	2.36	0.48	1.40	0.20	1.28	0.19
	0.75	25.64	50.65	6.08	23.59	4.41	1.07	4.11	0.58	2.83	0.53	1.57	0.21	1.44	0.22
	1.25	26.29	53.15	6.34	24.59	4.74	1.11	4.41	0.59	2.93	0.56	1.59	0.25	1.47	0.23
	1.75	22.46	44.37	5.37	20.50	3.96	0.92	3.63	0.49	2.46	0.47	1.40	0.20	1.26	0.19
	2.25	25.16	49.37	6.10	23.64	4.41	0.99	4.00	0.56	2.73	0.53	1.56	0.22	1.43	0.21
	2.75	22.55	45.61	5.49	21.31	4.09	0.94	3.73	0.50	2.60	0.48	1.39	0.20	1.26	0.18
	3.25	23.41	46.55	5.65	20.93	3.96	0.97	3.88	0.57	2.87	0.54	1.60	0.23	1.47	0.22
	3.75	21.65	44.23	5.21	19.55	3.58	0.87	3.53	0.49	2.52	0.50	1.50	0.21	1.37	0.21
	4.25	25.15	49.33	5.96	22.54	4.32	1.04	4.02	0.60	3.02	0.61	1.78	0.29	1.58	0.28
	4.75	27.73	54.67	6.63	25.19	4.93	1.15	4.36	0.61	3.04	0.57	1.69	0.23	1.50	0.23
	5.50	26.91	52.62	6.45	24.75	4.61	1.09	4.36	0.58	2.94	0.54	1.64	0.23	1.51	0.23
	6.50	25.63	51.02	6.18	23.63	4.48	1.07	4.22	0.58	2.86	0.59	1.59	0.22	1.57	0.21
	7.50	24.53	46.06	5.79	22.13	3.98	0.92	3.77	0.53	2.73	0.52	1.57	0.22	1.40	0.21
	9.00	16.48	32.86	3.80	14.32	2.78	0.67	2.62	0.40	1.97	0.40	1.15	0.19	1.06	0.17
	11.00	25.84	49.15	6.17	23.64	4.54	1.05	4.11	0.58	2.85	0.55	1.62	0.23	1.44	0.23
	13.00	21.69	42.19	5.04	19.33	3.65	0.86	3.42	0.50	2.56	0.49	1.50	0.20	1.40	0.21

redox reactions governed by the preferential use of the electron acceptor that yields the highest amount of free energy for the bacterially mediated oxidation of organic matter. Oxygen is reduced near the sediment–water interface, followed by the reduction of nitrate and manganese-oxide, then reactive iron oxide, and sulphate (Froelich et al., 1979; Postma and Jakobsen, 1996).

3.3. Vertical distribution of rare earth elements

The particulate content of REEs is listed in Tables 2 and 3. Although the 14 REEs were measured, only two REE profiles are shown. These are Ce and Eu presented in Figs. 6 and 7, respectively. Cerium and europium have been chosen because they may be expected to behave differently from the others REEs due to change in their oxidation states in specific environments (De Baar et al., 1985; Sholkovitz et al., 1994; Klinkhammer et al., 1994).

3.3.1. Total REEs content

The profiles of individual REEs mirror the one for Ce_{tot} (Fig. 6). The total REEs-content was between 0.11 ± 0.04 μg g^{-1} for Lu and 47.79 ± 4.10 μg g^{-1} for Ce (Table 2). The vertical profiles of the target elements showed little changes with depth in the sediments from the stations B and I (Figs. 6 and 7). However, we note two opposite trends in the cores collected at sites A and D. In core D, we observe an increase (~33%) of the average total REEs content below the oxic horizon (Table 2, Fig. 6). In contrast, the REEs-concentrations decrease in the bottom of the core A (below 14 cm). The highest S_{tot} content and the presence of Fe-monosulphides in the anoxic sediments of station D suggest the possibility that sulphides are a burial phase for REEs. Precipitation of pure REEs sulphides has never been reported and can probably be ruled out. Co-precipitation of the REEs with metal sulphides may be a valid explanation. Such process has already been reported by Schijf et al. (1995) to explain dissolved REEs distribution in the anoxic brines of the Bannock basin. Despite the lack of high S_{tot}-content in cores from the deepest stations (B, A, and I), the presence of small black dots at the surface of the sediment slices suggest trace quantities of FeS (Chaillou et al., 2003). Nevertheless, the REEs-concentrations remain constant at stations B and I. The possibility of a transfer from a previous phase, stable in the oxic horizon, to another phase associated to sulphides species may explain these observations. This is supported by the concomitant decrease of REEs concentrations and S_{tot} content (Fig. 5) in the bottom part of station A. Total REEs contains REEs phases which are sensitive to the presence of sulphides species. In addition, a threshold level of dissolved sulphide seems to be a prerequisite for the formation of a significant amount of an additional "authigenic" REEs, as indicated by the total REEs content profile at station D. Note that in this paper we define "authigenic" REEs as REEs that are taken up by the sediment (perhaps from the porewaters) in excess of those that were deposited at the sediment–water interface.

Following common practice, Fig. 8 shows NASC-normalized REEs concentration patterns for each core. Selected samples have been chosen in oxic and anoxic horizons. Fig. 8 reveals no significant change of patterns between the two redox conditions in the deepest

Table 3
Results of REEs extracted by an asorbate solution ($REEs_{asc}$) in μg g^{-1} in the modern sediments of the Bay of Biscay

	Depth (cm)	La	Ce	Pr	Nd	Sm	Eu	Gd	Tb	Dy	Ho	Er	Tm	Yb	Lu
Station D	0.25	2.05	5.12	0.72	2.59	0.67	0.55	0.76	0.08	0.56	0.06	0.23	0.02	0.17	0.02
	0.75	2.98	7.51	1.00	3.39	0.81	0.71	0.92	0.09	0.61	0.07	0.25	0.02	0.18	0.02
	1.25	3.00	7.51	0.99	3.46	0.83	0.72	0.91	0.09	0.63	0.07	0.25	0.02	0.18	0.02
	1.75	2.96	7.39	0.99	3.50	0.84	0.69	0.88	0.08	0.59	0.07	0.23	0.02	0.18	0.02
	2.50	2.97	7.59	1.02	3.55	0.84	0.73	0.88	0.09	0.61	0.07	0.24	0.02	0.19	0.02
	3.50	2.81	7.19	0.97	3.47	0.80	0.67	0.82	0.08	0.57	0.07	0.22	0.02	0.17	0.02
	4.50	2.90	7.30	0.98	3.35	0.80	0.71	0.91	0.08	0.61	0.07	0.24	0.02	0.18	0.02
	5.50	3.00	7.64	1.00	3.43	0.84	0.72	0.96	0.09	0.62	0.07	0.26	0.02	0.18	0.02
	6.50	2.97	7.59	0.99	3.36	0.80	0.69	0.93	0.08	0.63	0.07	0.25	0.02	0.18	0.02
	8.00	3.10	8.03	1.06	3.53	0.84	0.76	0.98	0.09	0.65	0.08	0.27	0.02	0.19	0.02
	10.00	2.87	7.51	0.97	3.16	0.78	0.70	0.90	0.08	0.59	0.07	0.24	0.02	0.17	0.02
	12.00	3.03	7.59	1.04	3.60	0.87	0.75	0.95	0.09	0.64	0.07	0.26	0.02	0.19	0.02
	16.00	3.23	8.18	1.10	3.74	0.94	0.79	1.00	0.09	0.70	0.08	0.28	0.03	0.20	0.02
	20.00	3.08	7.66	1.04	3.56	0.88	0.75	0.94	0.09	0.64	0.07	0.26	0.02	0.19	0.02
	24.00	3.05	7.36	1.02	3.53	0.85	0.72	0.91	0.08	0.62	0.07	0.25	0.02	0.17	0.02
	28.00	3.57	8.68	1.20	4.07	0.95	0.84	1.01	0.10	0.69	0.08	0.28	0.03	0.20	0.02
	32.00	3.49	8.60	1.20	4.10	1.00	0.85	1.05	0.10	0.71	0.08	0.29	0.03	0.21	0.02
	38.00	3.85	9.57	1.31	4.51	1.10	0.93	1.11	0.11	0.77	0.09	0.32	0.03	0.21	0.02
Station B	0.25	2.01	5.28	0.70	2.46	0.60	0.52	0.65	0.06	0.46	0.06	0.19	0.02	0.15	0.02
	0.75	1.85	4.94	0.63	2.23	0.53	0.52	0.59	0.06	0.43	0.05	0.19	0.02	0.14	0.01
	1.25	1.71	4.67	0.59	2.16	0.51	0.45	0.56	0.06	0.40	0.05	0.17	0.01	0.13	0.01
	1.75	1.75	4.61	0.59	2.14	0.52	0.44	0.56	0.06	0.40	0.05	0.18	0.02	0.14	0.01
	2.50	1.81	4.78	0.64	2.24	0.56	0.47	0.59	0.06	0.43	0.05	0.18	0.02	0.13	0.01
	3.50	1.69	4.52	0.60	2.03	0.51	0.45	0.57	0.05	0.41	0.05	0.18	0.01	0.13	0.01
	4.50	1.49	4.09	0.54	1.81	0.47	0.42	0.52	0.05	0.38	0.04	0.16	0.01	0.11	0.01
	5.50	1.50	4.12	0.55	1.84	0.49	0.42	0.53	0.05	0.39	0.04	0.16	0.01	0.11	0.01
	6.50	1.36	3.77	0.50	1.70	0.46	0.38	0.48	0.05	0.36	0.04	0.15	0.01	0.10	0.01
	8.00	1.43	3.77	0.52	1.83	0.45	0.38	0.50	0.05	0.35	0.04	0.15	0.01	0.11	0.01
	10.00	1.35	3.56	0.49	1.70	0.42	0.36	0.47	0.05	0.34	0.04	0.14	0.01	0.10	0.01
	12.00	1.34	3.45	0.48	1.67	0.39	0.36	0.46	0.04	0.32	0.04	0.14	0.01	0.10	0.01
	16.00	1.35	3.47	0.48	1.68	0.40	0.33	0.46	0.04	0.31	0.04	0.13	0.01	0.10	0.01
	20.00	1.37	3.49	0.49	1.74	0.39	0.36	0.50	0.05	0.33	0.04	0.13	0.01	0.11	0.01
	24.00	1.34	3.55	0.50	1.73	0.43	0.37	0.51	0.04	0.34	0.04	0.14	0.01	0.11	0.01
	28.00	1.11	2.91	0.41	1.43	0.36	0.31	0.40	0.04	0.29	0.03	0.12	0.01	0.09	0.01
	32.00	1.13	2.91	0.41	1.43	0.39	0.31	0.42	0.04	0.30	0.04	0.13	0.01	0.09	0.01
	38.00	1.03	2.57	0.36	1.30	0.33	0.28	0.38	0.04	0.27	0.03	0.12	0.01	0.09	0.01
Station A	0.25	2.23	5.29	0.71	2.41	0.57	0.52	0.66	0.06	0.50	0.06	0.22	0.02	0.17	0.02
	0.75	2.60	6.29	0.84	2.82	0.65	0.57	0.78	0.07	0.59	0.07	0.25	0.03	0.20	0.02
	1.25	2.32	5.56	0.76	2.57	0.64	0.56	0.73	0.07	0.52	0.07	0.25	0.02	0.18	0.02
	1.75	2.47	5.86	0.81	2.86	0.67	0.60	0.76	0.07	0.57	0.07	0.26	0.03	0.19	0.02
	2.25	2.26	5.35	0.75	2.64	0.63	0.53	0.73	0.07	0.53	0.06	0.24	0.02	0.18	0.02
	2.75	2.29	5.23	0.75	2.64	0.61	0.53	0.73	0.07	0.51	0.07	0.24	0.02	0.17	0.02
	3.50	2.14	4.88	0.72	2.45	0.58	0.51	0.68	0.06	0.48	0.06	0.22	0.02	0.17	0.02
	4.50	1.71	3.94	0.61	2.10	0.51	0.46	0.60	0.06	0.43	0.05	0.21	0.02	0.16	0.02
	5.50	1.58	3.73	0.58	2.11	0.51	0.46	0.58	0.06	0.43	0.06	0.20	0.02	0.15	0.02
	6.50	1.55	3.64	0.58	1.99	0.49	0.45	0.58	0.05	0.40	0.05	0.20	0.02	0.15	0.02
	8.00	1.38	3.27	0.52	1.84	0.43	0.42	0.53	0.05	0.38	0.05	0.18	0.02	0.13	0.02
	10.00	1.32	3.16	0.51	1.74	0.42	0.39	0.53	0.05	0.37	0.05	0.17	0.02	0.14	0.02
	12.00	1.36	3.17	0.51	1.88	0.46	0.42	0.53	0.05	0.40	0.05	0.19	0.02	0.15	0.02
	14.00	1.38	3.16	0.52	1.87	0.47	0.41	0.54	0.05	0.41	0.05	0.18	0.02	0.14	0.02
	18.00	1.18	2.64	0.45	1.69	0.42	0.37	0.47	0.05	0.37	0.05	0.17	0.02	0.13	0.02
	22.00	1.15	2.58	0.45	1.67	0.41	0.38	0.47	0.05	0.37	0.04	0.17	0.02	0.13	0.01
Station I	0.25	3.64	9.21	1.12	3.82	0.86	0.81	1.03	0.09	0.72	0.09	0.33	0.03	0.23	0.03
	0.75	3.32	8.41	1.05	3.64	0.81	0.76	0.96	0.09	0.66	0.08	0.31	0.03	0.24	0.03
	1.25	3.38	8.71	1.07	3.77	0.83	0.77	0.99	0.09	0.70	0.09	0.32	0.03	0.24	0.03
	1.75	3.37	8.79	1.07	3.81	0.84	0.79	0.99	0.09	0.67	0.09	0.31	0.03	0.24	0.03
	2.25	3.39	8.49	1.09	3.61	0.81	0.78	0.96	0.09	0.68	0.08	0.30	0.03	0.23	0.03
	2.75	3.53	8.67	1.11	3.76	0.83	0.81	0.95	0.09	0.70	0.09	0.31	0.03	0.24	0.03

Table 3 (*continued*)

	Depth (cm)	La	Ce	Pr	Nd	Sm	Eu	Gd	Tb	Dy	Ho	Er	Tm	Yb	Lu
Station I	3.25	3.31	8.28	1.03	3.46	0.79	0.72	0.87	0.08	0.65	0.08	0.29	0.03	0.22	0.02
	3.75	3.51	8.67	1.08	3.58	0.82	0.75	0.92	0.09	0.69	0.08	0.31	0.03	0.23	0.03
	4.25	3.13	7.46	0.95	3.25	0.73	0.69	0.81	0.08	0.61	0.07	0.27	0.03	0.20	0.02
	4.75	3.12	7.28	0.99	3.23	0.74	0.71	0.84	0.08	0.62	0.08	0.29	0.03	0.22	0.02
	5.50	2.65	6.29	0.86	2.92	0.66	0.62	0.75	0.07	0.54	0.07	0.24	0.02	0.19	0.02
	6.50	2.35	5.64	0.80	2.74	0.65	0.59	0.72	0.07	0.50	0.06	0.24	0.02	0.18	0.02
	7.50	2.37	5.61	0.79	2.77	0.63	0.62	0.72	0.07	0.52	0.06	0.25	0.02	0.18	0.02
	9.00	2.33	5.87	0.82	2.75	0.66	0.59	0.74	0.07	0.50	0.06	0.24	0.02	0.18	0.02
	11.00	2.25	5.71	0.74	2.53	0.56	0.55	0.65	0.06	0.47	0.06	0.22	0.02	0.16	0.02
	13.00	2.12	5.53	0.72	2.47	0.56	0.54	0.65	0.06	0.47	0.06	0.22	0.02	0.16	0.02

stations. On the contrary, NASC normalized REEs concentrations of the anoxic sample are the highest in the core D. For station A, two distinct samples located above (10 cm) and inside (22 cm) the S_{tot} depleted sediment layer have been chosen. As for stations B and I, the pattern of the first sample superimposes the superficial sample. In the contrary, NASC-normalized REEs data of the S_{tot} depleted sample are lower. These results corroborate the importance of metal sulphides as a possible carrier phase for particulate REEs in modern sediments. The shapes of NASC-normalized REE patterns in oxic and anoxic horizons are similar and show weak negative distribution slopes, being slightly depleted in a linear fashion from La to Lu. This is consistent with a relative enrichment of light REEs (from La to Sm) over heavy REEs (from Gd to Lu) probably due to the preferential absorption (or scavenging) of these light elements compared to their heavy neighbors (e.g. Elderfield, 1988). The preferential adsorption with decreasing atomic number has been attributed to the decreasing stability of solvated trivalent cations (Byrne and Kim, 1990). The vertical distributions of Er/Nd (Fig. 9), an index of heavy REEs enrichment (Elderfield and Sholkovitz, 1987), show also no vertical change or differences between cores. The observed values between and within cores (0.06831 ± 0.0007) are close to the Er/Nd NASC ratio (0.08). Neither Ce nor Eu anomalies are formed ($Ce/Ce^* \sim 1$, $Eu/Eu^* \sim 1$, with $Ce/Ce^* = 3(Ce/Ce_{shale})/(2(La/La_{shale}) + (Nd/Nd_{shale}))$, and $Eu/Eu^* = (Eu/Eu_{shale})/((Sm/Sm_{shale}) \times (Gd/Gd_{shale}))^{1/2}$) confirming the homogeneous behavior of the lanthanides with sediment depth. However, a weak positive anomaly of Gd is observed (Fig. 8) and appeared to be characteristic of these muddy sediments (Jouanneau et al., 1998). In these modern sediments, the observed fractionation of the lanthanide series is not governed by the redox conditions but is linked to the sediment sources.

3.3.2. Ascorbate reactive REEs content

Although the behavior of REEs is poorly understood (Byrne and Biqiong, 1995), it is assumed that adsorption on clay minerals is the main factor controlling their

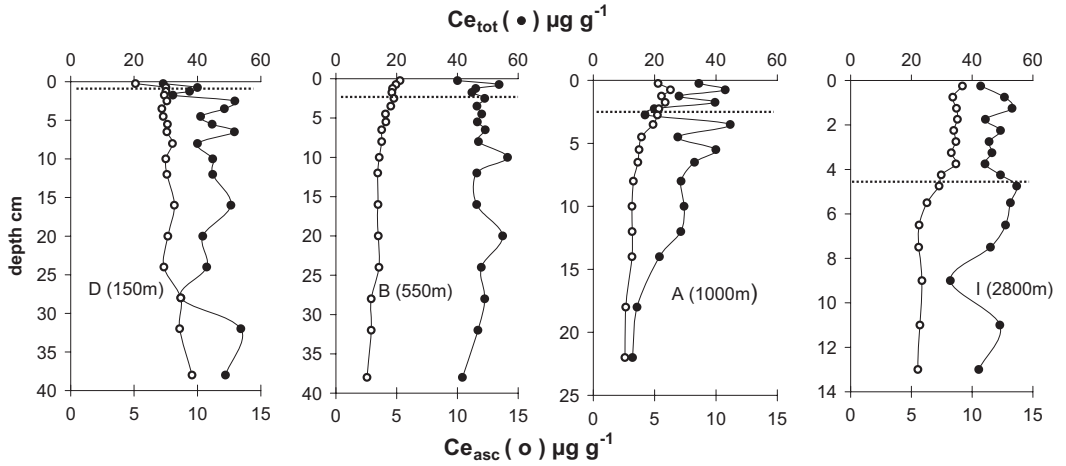

Fig. 6. Concentrations (in µg g^{-1}) of ascorbate extractable Ce (Ce_{asc}, ○) and total Ce (Ce_{tot}, ●) vs. depth at stations D (150 m), B (550 m), A (1000 m) and I (2800 m). Dashed lines represent the depth of the O_2 front.

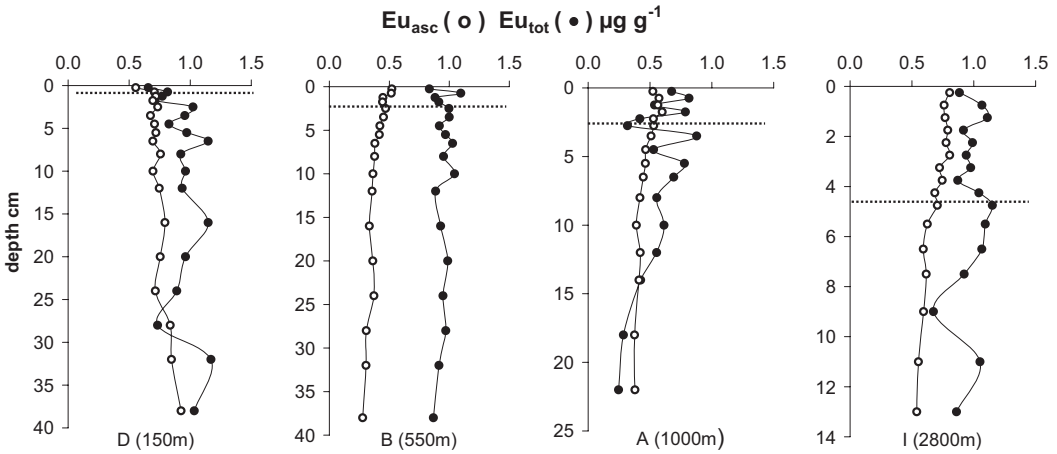

Fig. 7. Concentrations (in µg g^{-1}) of ascorbate extractable Eu (Eu_{asc}, ○) and total Eu (Eu_{tot}, ●) vs. depth at stations D (150 m), B (550 m), A (1000 m) and I (2800 m). Dashed lines represent the depth of the O_2 front.

sedimentary geochemistry (Bradbury and Baeyens, 2002; Coppin et al., 2002). Several studies in various environments (open ocean, anoxic brines, OMZ, estuaries) have shown that the reactive solid phase REEs are dominantly in particulate coatings composed of Mn, Fe oxides or Fe–Mn oxides, organic matter and metal sulphides (De Baar et al., 1985; Byrne and Kim, 1990; German et al., 1991; Sholkovitz et al., 1994; Elbaz-Poulichet and Dupuy, 1999; Kuss et al., 2001; De Carlo and Green, 2002; Bozau et al., 2004; Haley et al., 2004).

The ascorbate extraction let us determine whether adsorption on the most reducible part of Fe- and Mn-oxides and Fe-monosulphides is significant in these sediments. The Ce_{asc} profiles (Fig. 6) are an example of vertical distributions of REEs extracted by ascorbate in these sediments. Ascorbate extractable REEs were highest in the metal oxides enriched horizons of stations B, A, and I (Table 3). Below this enrichment, the REE_{asc} content decreased progressively to reach constant values. At station D, the REE_{asc} concentrations increase with sediment depth (Table 3; Fig. 6). The vertical distribution of $(Er/Nd)_{asc}$ ratio was nearly constant (Fig. 9), indicating a similar behavior of reactive REEs with depth. In the top of the cores, ascorbate extractable REE was 15% and 20% of the total for all the REEs, except Eu, and less than 10% near the bottom. Because this reducible fraction is small, it does not affect significantly the total REE signal. We observe no REE_{asc} peaks, unlike Mn_{asc} and Fe_{asc} (Figs. 4 and 6). In this respect, REEs differ from other trace elements. The ascorbate extractable fraction of such elements, for example Mo or As, is similar to ascorbate extractable Mn and Fe (Chaillou et al., 2002, 2003). The absence of peak in extractable REEs indicates that authigenic metal oxides do not scavenge dissolved REEs, and/or that REEs are not mobilized in reducing sediment. The first hypothesis suggests that the surficial enrichment of REE_{asc} is not diagenetic but detrital. REEs associated to ascorbate reactive particles in the water column accumulate by hemipelagic sedimentation. This is consistent with the well known ability of metal oxides to efficiently scavenge water column REEs. These ascorbate reactive particles can be freshly Fe- and Mn-oxides formed in the water column. Their reductive dissolution below the oxic horizon should mobilize adsorbed REEs to reducing porewaters. The second hypothesis is supported by the observations of Sholkovitz et al. (1992) who found no correlation between the release of REE and the release of Fe and Mn in the upper porewater of the sediments. This idea corroborates a direct transfer of two solid REEs phases without mobilization in porewaters.

At station D, the increase of REE_{asc} is parallel to the profiles of S_{tot} and Fe_{asc} (Figs. 4–6). Like total solid REEs, the master variable regulating REE_{asc} content thus could be the production of Fe-monosulphides or dissolved sulphides. A first critical sulphides concentration seems prerequisite to explain the active formation of reactive REEs, probably by co-precipitation of REE–Fe–S phase. Nevertheless this reactive fraction appears too weak to explain the total REEs increase suggesting the ascorbate solution is unable to extract the totality of the additional “authigenic” REEs fraction.

The vertical profiles of Eu_{asc} (Fig. 7) parallel the profiles of the other ascorbate extractable REEs. They are weakly enriched in the oxic layer relative to a background concentration measured down the cores. However, the background concentration of europium

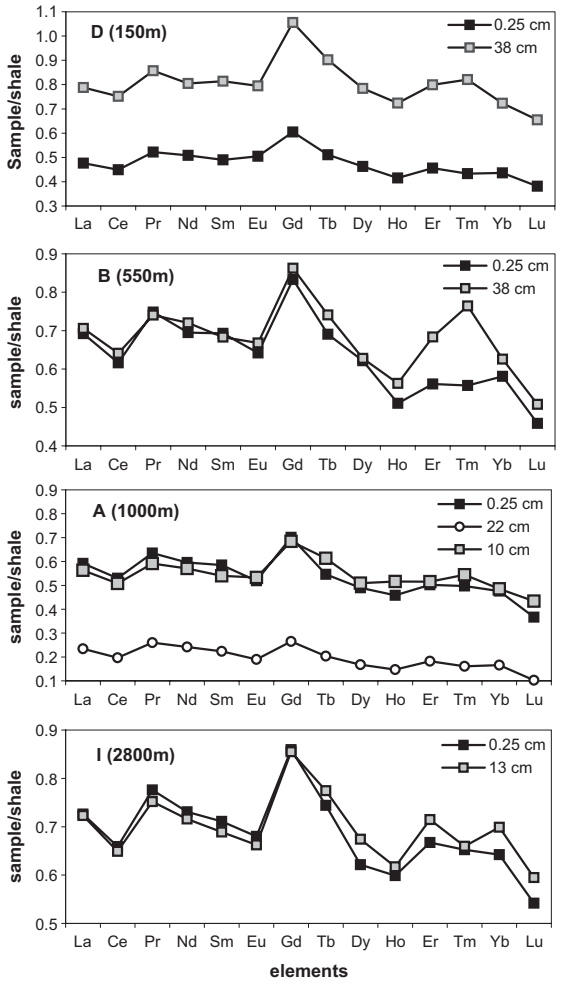

Fig. 8. Distribution patterns of REE normalized to North American Shale Composite (Gromet et al., 1984) for selected samples from the oxic and anoxic horizons of the sediment cores. Samples have been chosen from the top of sediment cores (0–0.5 cm), enriched in metal oxides; and samples from the bottom of cores (37–39 cm for stations D and B, 9–10 and 21–23 for station A, and 12–14 cm for station I), enriched in sulphide species.

extracted with ascorbate contributed to more than 50% of the total Eu (Fig. 7) suggesting enhanced solubilization of Eu in the reductive ascorbate solution. Although Eu^{3+}/Eu^{2+} equilibria is highly temperature dependent (Sverjensky, 1984), the thermodynamic data (pe^o) indicate that Eu reduction is favorable at the pH and temperature of the sea water. Europium is reduced at a lower potential of Fe, as observed MacRae et al. (1992), thus under reducing and neutral pH conditions, Eu^{3+} should be reduce to Eu^{2+} by the ascorbate solution, in a manner analogous to that in which ascorbate reduces Fe^{3+} to Fe^{2+}. Whereas other REEs keep their valency constant (+III) during the ascorbate leaching, Eu(III) could be reduced as Eu(II) and then be dissolved in the leaching solution. Eu(II) is more soluble than Eu(III) and must be easily desorbed from the carrier phase during the ascorbate leaching. The Eu(III), which is leached can not be strongly bound within refractory mineral lattices, but is likely adsorbed on particle surfaces. The other REE(III) must occur at the same sites than Eu(III). This result highlights the non-reducible nature of the reactive REEs phase formed in sulphidic sediments. Mobilization and precipitation of a reactive REEs fraction as REE–Fe–S or REE–S directly phase needs further considerations.

4. Summary

In modern sediments of the Bay of Biscay, the geochemical behavior of total REEs appears to be affected by the presence of metal sulphides. In deeper sites where sulphate reduction is weak, sulphides appear to be an important burial phase for total solid REEs. Here, the transfer of REEs from an unknown previous phase, stable in oxic conditions, to another one associated with sulphides seems to be direct, without mobilization in porewaters. In contrast, in sediments where greater sulphate reduction occurs, the formation of an additional "authigenic" fraction is observed. There was no Ce and Eu anomaly linked to diagenetic processes of organic matter mineralization, and the Er/Nd ratio remained constant and close to the shale ratio. There is no fractionation in the lanthanide series related to changes of redox conditions. The linear pattern across the series and the Gd anomaly reflects the detrital sediment sources, originating from the Atlantic coastal zone.

The content of ascorbate extractable REEs is small and the surficial enrichment of REE_{asc} does not affect the total sedimentary signal. We observe no direct relationship between the REE_{asc} profiles and the profiles of authigenic metal-oxides. This indicates that the major reducible phase of Fe- and Mn-oxides do not act as efficient REEs traps in the sediment. This surficial enrichment could correspond to REEs co-precipitated, or scavenged onto detrital Fe- and Mn-oxides that settled on the sediment. Our results do not permit us to make a distinction between the relative importance of Fe- and Mn-oxides as REEs carrier phases. When oxides are reduced at depth, the absorbed REEs are transferred to another unidentified particle phase.

In the modern sediments of the Bay of Biscay, the particulate REEs are weakly mobile. Nevertheless, a threshold level of sulphides appears to promote the formation of an "authigenic" REEs fraction, with a non-reducible nature. The use of particulate REEs as geochemical tracers might be impacted by early diage-

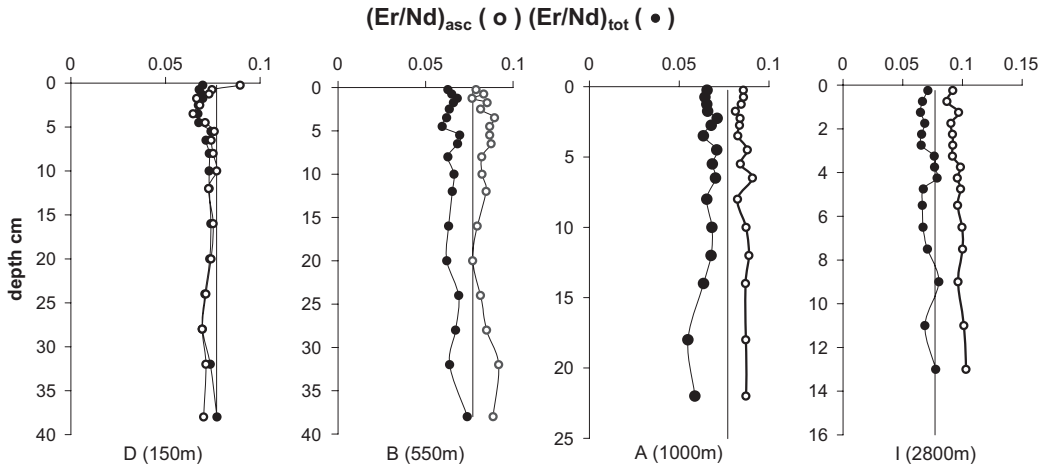

Fig. 9. Vertical profiles of ascorbate extractable Er/Nd ratio (○) and total Er/Nd ratio (●) at stations D (150 m), B (550 m), A (1000 m) and I (2800 m). The full line represents the shale ratio (0.08).

netic processes and particularly in sediments where sulphides production is efficient. The formation of an "authigenic" REEs phase, as REE–Fe–S or REE–S in modern sediments needs further investigation and in this respect, future studies using REEs as biogeochemical tracers are needed.

Acknowledgements

This research was funded by the program PROOF of the Institut National des Sciences de l'Univers. We gratefully acknowledge the assistance of the crew of the "Côte de la Manche" and the participants of the Oxybent missions. We would like to express our gratitude to Pr. Bjørn Sundby for English correction and his helpful comments. Also acknowledged are the very useful pre-review of Dr. M. Zabel and one anonymous reviewer. E. Sholkovitz and K.H. Jonhannesson are gratefully acknowledged for their useful comments and suggestions. Gwénaëlle Chaillou expresses her special gratitude to Pr. D. Burdige, who worked hard to review the manuscript.

References

Aagaard, P., 1974. Rare earth elements adsorption on clay minerals. Bulletin Groupe Français des Argiles, t XXVI, 193–199.

AFNOR, 1997. Dictionnaire de l'Environnement, recueil des Normes françaises, 2éme édition. AFNOR édition, Paris.

Anschutz, P., Zhong, S., Sundby, B., Mucci, A., Gobeil, C., 1998. Burial efficiency of phosphorus and the geochemistry of iron in continental margin sediment. Limnol. Oceanogr. 43, 53–64.

Arraes-Mescoff, R., Roy-Barman, M., Coppola, L., Souhaut, M., Tachikawa, K., Jeandel, C., Sempere, R., Yoro, C., 2001. The behavior of Al, Mn, Ba, Sr, REE and Th isotopes during in vitro degradation of large marine particles. Mar. Chem. 73, 1–19.

Balashov, Y.A., Girin, Y.P., 1969. On the reserve of mobile rare earth elements in sedimentary rocks. Geochem. Int. 6, 951–969.

Berner, R.A., 1970. Sedimentary pyrite formation. Am. J. Sci. 268, 1–23.

Bozau, E., Leblanc, M., Seidel, J.L., Stärk, H.J., 2004. Light rare earth element in an acidic mine lake (Lusatia, Germany). Appl. Geochem. 19, 261–271.

Bradbury, M.H., Baeyens, B., 2002. Sorption of Eu on Na- and Ca-montmorillonites: experimental investigations and modelling with cation exchange and surface complexation. Geochim. Cosmochim. Acta 66 (13), 2325–2334.

Broecker, W.S., Peng, T.H., 1982. Tracers in the sea. Columbia University, Palisades.

Byrne, R.H., Kim, K.H., 1990. Rare earth element scavenging in seawater. Geochim. Cosmochim. Acta 54, 2645–2656.

Byrne, R.H., Biqiong, L., 1995. Comparative complexation behavior of the rare earths. Geochim. Cosmochim. Acta 59 (22), 4575–4589.

Chaillou, G., Anschutz, P., Lavaux, G., Schäfer, J., Blanc, G., 2002. The distribution of Mo, U and Cd in relation to major redox species in muddy sediments of the Bay of Biscay. Mar. Chem. 80, 41–59.

Chaillou, G., Schäfer, J., Anschutz, P., Lavaux, G., Blanc, G., 2003. The behavior of Arsenic in muddy sediments of Bay of Biscay (France). Geochim. Cosmochim. Acta 67 (16), 2993–3003.

Coppin, F., Berger, G., Bauer, A., Castet, S., Loubet, M., 2002. Sorption of lanthanides on smectite and kaolinite. Chem. Geol. 182, 57–68.

De Baar, H.J.W., Bacon, M.P., Brewer, P.G., Bruland, K.W., 1985. Rare-earth elements in the Pacific and in the Atlantic Oceans. Geochim. Cosmochim. Acta 49, 1953–1959.

De Carlo, E.H., Green, W.J., 2002. Rare earth element in the water column of Lake Vanda, McMurdo dry valleys Antarctica. Geochim. Cosmochim. Acta 66, 1323–1333.

Elbaz-Poulichet, F., Dupuy, C., 1999. Behavior of rare earth elements at the freshwater–seawater interface of two acid mine rivers: the Tinto and Odiel (Andalucia, Spain). Appl. Geochem. 14, 1063–1072.

Elderfield, H., Greaves, M.J., 1982. The rare earth elements in seawater. Nature 296, 214–219.
Elderfield, H., Pagett, R., 1986. Rare Earth Elements in Ichthyoliths: variations with redox conditions and depositional environments. Sci. Total Environ. 49, 175–197.
Elderfield, H., Sholkovitz, E.R., 1987. Rare Earth Elements in the porewater of reducing nearshore sediments. Earth Planet. Sci. Lett. 82, 280–288.
Elderfield, H., 1988. The oceanic chemistry of the rare earth elements. Philos. Trans. R. Soc. Lond., A 325, 105–126.
Elderfield, H., Upstill-Goddard, R., Sholkovitz, E.R., 1990. The rare earth elements in rivers, estuaries, and coastal seas and their significance to composition of ocean waters. Geochim. Cosmochim. Acta 54, 971–991.
Fleet, A.J., 1984. Aqueous and sedimentary geochemistry of the rare earth elements. In: Henderson, P. (Ed.), Rare Earth Elements Geochemistry. Elsevier, Amsterdam, pp. 343–373.
Froelich, P.N., Klinkhammer, G.P., Bender, M.L., Luedke, N.A., Heath, G.R., Cullen, D., Dauphin, P., Hammond, D., Hartman, B., Maynard, V., 1979. Early oxidation of organic matter in pelagic sediments of the Eastern Equatorial Atlantic: suboxic diagenesis. Geochim. Cosmochim. Acta 43, 1075–1090.
German, C.R., Holliday, B.P., Elderfield, H., 1991. Redox cycling of rare earth elements in the suboxic zone of the Black Sea. Geochim. Cosmochim. Acta 55, 3553–3558.
German, C.R., Hergt, J., Palmer, M.R., Edmond, J.M., 1999. Geochemistry of a hydrothermal sediment core from the OBS vent-field, 21°N East Pacific Rise. Chem. Geol. 155 (1–2), 65–75.
Goldstein, S.J., Jacobsen, S.B., 1987. The Nd and Sr isotopic systematic of river–water dissolved material: implications for the sources of Nd and Sr in seawater. Chem. Geol. 66, 245–272.
Gromet, L.P., Dymeck, R.F., Haskin, L.A., Korotev, R.L., 1984. The North American shale composite: compilation major and trace elements characteristics. Geochim. Cosmochim. Acta 48, 2469–2482.
Grousset, F.E., Parra, M., Bory, A., Martinez, P., Bertrand, P., Shimmiled, G., Ellam, R.M., 1998. Saharan wind regimes traced by the Sr–Nd isotopic compositions of the subtropical Atlantic sediments: last glacial maximum vs. today. Quat. Sci. Rev. 17, 395–409.
Haley, B.A., Klinkhammer, G.P., McManus, J., 2004. Rare earth elements in pore waters of marine sediments. Geochim. Cosmochim. Acta 68, 1265–1279.
Henderson, P., 1984. Rare Earth Element Geochemistry. Elsevier, Amsterdam.
Hyacinthe, C., Anschutz, P., Jouanneau, J.-M., Jorissen, F.J., 2001. Early diagenesis processes in the muddy sediment of the Bay of Biscay. Mar. Geol. 177, 111–128.
Jørgensen, B.B., 1982. Mineralization of organic matter in the seabed. The role of the sulfate reduction. Nature 296, 643–645.
Jouanneau, J.M., Weber, O., Grousset, F.E., Thomas, B., 1998. Pb, Zn, Cs, Sc and rare earth elements as tracers of the Loire and Gironde particles on the Biscay shelf (SW France). Oceanol. Acta 21 (2), 233–241.
Klinkhammer, G., German, C.R., Elderfield, H., Greaves, M.J., Mitra, A., 1994. Rare earth elements in hydrothermal fluids and plume particulates by inductively coupled plasma mass spectrometry. Mar. Chem. 45, 179–186.
Kostka, J.E., Luther III, G.W., 1994. Portioning and speciation of solid phase iron in saltmarsh sediments. Geochim. Cosmochim. Acta 58, 1701–1710.
Kuss, J., Garbe-Schönberg, C.D., Kremling, K., 2001. Rare earth elements in suspended particulate material of North Atlantic surface waters. Geochim. Cosmochim. Acta 65 (2), 187–199.
Latouche, C., Jouanneau, J.M., Lapaquellerie, Y., Maillet, N., Weber, O., 1991. Répartition des minéraux argileux sur le plateau continental Sud-Gascogne. Oceanol. Acta 11, 155–161.
Loring, D.H., Rantala, R.T.T., 1992. Manual for the geochemical analysis of marine sediment and suspended particulate matter. Earth Sci. Rev. 32, 235–283.
McLennan, S.M., 1989. Rare earth elements in sedimentary rock: influence of provenance and sedimentary processes. In: Lipin, B.R., McKay, G.A. (Eds.), Geochemistry and Mineralogy of Rare Earth Elements, Reviews in Mineralogy, vol. 21. Mineral. Soc. Am, Washington, pp. 169–200.
MacRae, N.D., Nesbitte, H.W., Kronbergb, B.I., 1992. Development of a positive Eu anomaly during diagenesis. Earth Planet. Sci. Lett. 109 (3–4).
Murray, R.W., Ten Brick, M.R.B., Gerlach, D.C., Russ III, G.P., Jones, D.L., 1992. Interoceanic variation in the rare earth, major, and trace element depositional chemistry of chert: perspectives gained from the DSDP and ODP record. Geochim. Cosmochim. Acta 56, 1897–1913.
Olivarez, A.M., Owen, R.M., 1991. The europium anomaly of seawater: implications for fluvial versus hydrothermal REE inputs to the oceans. Chem. Geol. 92, 317–328.
Piper, D.Z., 1974. Rare earth elements in the sedimentary cycle: a summery. Chem. Geol. 14, 285–315.
Postma, D., Jakobsen, R., 1996. Redox zonation: equilibrium contains on the Fe(III)/SO4-reduction interface. Geochim. Cosmochim. Acta 60 (17), 3169–3175.
Revsbech, N.P., 1983. In-situ measurements of oxygen profiles of sediments by use of oxygen microelectrodes. In: Forstner, G. (Ed.), Polarographic Oxygen Sensors. Springer-Verlag, Berlin, pp. 265–273.
Schijf, J., De Baar, H.J.W., Millero, F.J., 1995. Vertical distributions and speciation of dissolved rare earth elements in the anoxic brines of Bannock Basin, eastern Mediterranean Sea. Geochim. Cosmochim. Acta 59 (16), 3285–3299.
Shields, G., Stille, P., 2001. Diagenetic constraints on the use of cerium anomalies as palaeoseawater redox proxies: an isotopic and REE study of Cambrian phosphorites. Chem. Geol. 175 (1–2), 29–48.
Sholkovitz, E.R., Elderfield, H., 1988. The cycling of dissolved rare-earth elements in Chesapeak Bay. Global Geochem. Cycles 2, 157–176.
Sholkovitz, E.R., 1992. Chemical evolution of rare earth elements: fractionation between colloidal and solution phases of filtered river water. Earth Planet. Sci. Lett. 114, 77–84.
Sholkovitz, E.R., Shaw, T.J., Schneider, D.L., 1992. The geochemistry of rare earth elements in the seasonally anoxic water column and porewaters of Chesapeak Bay. Geochim. Cosmochim. Acta 56, 3389–3402.
Sholkovitz, E.R., 1993. The geochemistry of rare earth elements in the Amazon River Estuary. Geochim. Cosmochim. Acta 57, 2181–2190.
Sholkovitz, E., Landing, W.M., Lewis, B.L., 1994. Ocean particle chemistry: the fractionation of the rare earth elements between suspended particles and seawater. Geochim. Cosmochim. Acta 58, 1567–1580.
Sinitsyn, V.A., Aja, S.U., Kulik, D.A., Wood, S.A., 2000. Acid–base surface and sorption of some lanthanides on K+-satured Marble-

head illite: I. Results of an experimental investigation. Geochim. Cosmochim. Acta 64 (2), 185–194.
Strickland, J.D.H., Parsons, T.R., 1972. A practical handbook of seawater analysis. Bull. Fish. Res. Board Can. 167, 1–31.
Sverjensky, D.A., 1984. Europium redox equilibria in aqueous solution. Earth Planet. Sci. Lett. 67, 70–78.
Tachikawa, K., Jeandel, C., Roy-Barman, M., 1999. A new approach to the Nd residence time in the ocean: the role of atmospheric inputs. Earth Planet. Sci. Lett. 170, 433–446.
Tauzin, P., 1974. Etude des relations entre les caractéristiques physico-chimiques et chimiques des milieux de dépôts et la distribution de quelques éléments métalliques dans les sédiments de divers environnements du Golfe de Gascogne. University Bordeaux I, Bordeaux. 120 pp.
Thomas, B., Besson, T., Quétel, C., Donard, O.F.X., Grouset, F.E., Monaco, A., Heussner, S., 1994. Biogeochemistry of Rare Earth Elements in suspended particulate matter from the water column of the Bay of Biscay. European Geophysical Society Meeting, Ann. Geophys., p. C246.